PHILOSOPHICAL TRANSACTIONS OF THE ROYAL SOCIETY A MATHEMATICAL, PHYSICAL & ENGINEERING SCIENCES

Intergranular Embrittlement in CrMoV Steels: An Assessment of the Effects of Residual Impurity Elements on High Temperature Ductility and Crack Growth

B. L. King

Phil. Trans. R. Soc. Lond. A 1980 **295**, 235-251
doi: 10.1098/rsta.1980.0104

Phil. Trans. R. Soc. Lond. A **295**, 235–251 (1980) [235]
Printed in Great Britain

Intergranular embrittlement in CrMoV steels: an assessment of the effects of residual impurity elements on high temperature ductility and crack growth

By B. L. King

Materials Division, Central Electricity Research Laboratories, Kelvin Avenue, Leatherhead, Surrey KT22 7SE, U.K.

[Plate 1]

Examination of the causes of cracking in the heat-affected zones of welded joints in CrMoV steels during stress relief or operation at elevated temperature has shown that the presence of certain residual impurity elements is an important contributory factor.

A detailed study of the effects of the elements P, As, Sn, Sb and Cu on the high temperature ductility and crack propagation behaviour of heat-affected zone microstructures in $\frac{1}{2}Cr\frac{1}{2}Mo\frac{1}{4}V$ steel has been carried out to provide information on the role of these elements in the formation of cracks during stress relief and their growth in service. Work on experimental alloys has identified the relative importance of individual elements in promoting intergranular embrittlement; comparison is made with the behaviour of commercial steels.

The results are discussed in terms of a possible embrittlement mechanism and consideration is given to the practical measures available for preventing cracking, both in terms of residual element and microstructure control.

1. Introduction

Low alloy steels of the $\frac{1}{2}Cr\frac{1}{2}Mo\frac{1}{4}V$ type (BS3604: HF/CD660 and similar) are widely used in the construction of power plant components for service up to 565C. However, fabrication and service experience has shown that these steels are susceptible to the formation of cracks in the heat-affected zones (h.a.zs) of welded joints during post-weld stress relieving heat treatments or during initial service life.

Examination of many examples of cracking has shown that the cracks are invariably intergranular and form within grain coarsened, bainitic, regions of the h.a.z. More detailed examination has shown that defects originate as planar arrays of discrete creep cavities on prior austenite boundaries in these regions and that these cavities grow and eventually link to form a network of intergranular cracks. At this stage the cracking is detectable by ultrasonic methods and can be rectified, although this is time consuming and costly. However, damage present only as cavitation or isolated microcracks at the time of inspection is more serious as it may not be detectable and may propagate in service. This is a particular danger in the h.a.z. of a butt weld where the growth of a circumferential crack can lead to joint severance and explosive failure. Consequently, there are strong incentives to identify and control the factors responsible for cracking to achieve greater plant safety and reduced repair and maintenance costs.

Recent studies of h.a.z. cracking in CrMoV steels have identified some aspects of the role of material composition, microstructure and residual stress (Schüller *et al.* 1974*a*, *b*; Batte *et al.*

1976; Myers & Price 1977). However, it is clear that cast-to-cast variations in composition are also important as some casts of steel are more susceptible than others, the contents of the main alloying elements being similar. These variations may originate in deoxidation practice where the use of Ti as a deoxidant has been shown to be preferable to Al in cast CrMoV steels (Myers 1972; Harris & Jones 1972) and this aspect is considered in more detail by Batte *et al.* in the following paper. Additionally, it has been shown that the susceptibility to cracking depends on the level of vanadium through its differing effects on the rupture strength of the h.a.z. and the parent material and, in particular, that high levels of V are detrimental (Myers 1979 and this symposium).

Significant compositional variations may also originate from impurities inherited from raw materials such as ore and scrap and which may persist during steelmaking. The elements of particular concern in this respect are P, As, Sn and Sb, which are known to embrittle prior austenite grain boundaries and to promote temper embrittlement (A.S.T.M. 1968, 1971) and Cu, which has been shown to cause 'hot shortness' (Melford 1962, 1966). Although it is clear that, in general, these elements promote high temperature failure in CrMoV steels (Hopkins *et al.* 1971; Tipler & Hopkins 1976; Tipler 1978), the evidence needed to identify their individual effects is lacking. Therefore, as the effective control of residual elements requires knowledge of their specific effects, this paper presents the results of high temperature ductility and crack propagation studies on a number of experimental and commercial $\frac{1}{2}$Cr$\frac{1}{2}$Mo$\frac{1}{4}$V steels to provide such information under conditions relevant to the formation and growth of h.a.z. cracks.

2. Materials

(*a*) *Experimental alloys*

Controlled additions of P, As, Sn, Sb and Cu were made to a range of experimental $\frac{1}{2}$Cr$\frac{1}{2}$Mo$\frac{1}{4}$V alloys. The compositions (table 1*a*) were based on the mean of the prevailing specification and the residual element additions corresponded either to the permitted maximum or, when not specified, to the maximum level likely to occur commercially. The alloys were based on Japanese electrolytic iron and were produced as 20 kg vacuum induction melted ingots which were subsequently forged and hot rolled to 25 mm square bar.

(*b*) *Commercial steels*

For comparative purposes a number of commercial CrMoV steels were also examined (table 1*b*). These steels, which embrace a wide range of residual element contents, were obtained from various steampipes and valve forgings, of which some of the latter are known to be susceptible to stress relief cracking as noted in table 1*b*.

3. Experimental procedure

(*a*) *High temperature strength and ductility*

The formation of cracks in the h.a.z. of a weld occurs when the local ductility is insufficient to accommodate the creep strains necessary to relax the residual welding stresses. Consequently, tensile ductility is considered to be indicative of the ease of formation of stress relief cracks. In the present work measurements were made at 550 °C, within the régime where impurity segregation effects are expected to be most marked and where the nucleation of stress relief cracks may occur.

PHILOSOPHICAL TRANSACTIONS OF THE ROYAL SOCIETY A MATHEMATICAL, PHYSICAL & ENGINEERING SCIENCES

Table 1. Alloy composition (percentages by mass)

(*a*) *Experimental alloys*

	C	Cr	Mo	V	Mn	Si	S	Al	Ni	P	As	Sn	Sb	Cu	
BS3604 / HF/CD660	0.08† / 0.15	0.25 / 0.50	0.50 / 0.70	0.22 / 0.30	0.40 / 0.70	0.10 / 0.35	0.04 (max.)	‡	0.30† (max.)	0.04 (max.)	—	0.02† (max.)	—	0.25† (max.)	
'pure' CMV	0.13	0.50	0.56	0.26	0.58	0.30	0.005	0.011	< 0.01	*0.002*	*0.002*	*0.001*	*0.001*	*0.018*	all alloys: Nb, Ti, W, Co < 0.01; B < 0.001
CMV + P	0.13	0.47	0.69	0.28	0.55	0.31	0.006	< 0.01	< 0.01	*0.042*	0.002	0.001	0.001	< 0.02	
CMV + As	0.10	0.48	0.55	0.20	0.56	0.28	0.008	< 0.01	< 0.01	0.003	*0.032*	0.001	0.001	< 0.02	
CMV + Sn	0.14	0.48	0.56	0.28	0.60	0.26	0.006	0.014	< 0.01	0.003	0.002	*0.027*	0.001	< 0.02	
CMV + Sb	0.10	0.53	0.58	0.28	0.60	0.31	0.008	< 0.01	< 0.01	0.003	0.002	0.001	*0.009*	< 0.02	
CMV + (P, As, Sn, Sb)	0.12	0.48	0.54	0.26	0.58	0.30	0.005	< 0.01	< 0.01	*0.037*	*0.037*	*0.028*	*0.016*	*< 0.02*	
CMV + Cu	0.16	0.45	0.49	0.26	0.58	0.28	0.005	< 0.01	< 0.01	0.002	0.002	0.001	0.001	*0.29*	

† Additional requirement of CEGB Standard 23584 (issue 3, June 1974).
‡ Maximum Al addition to be 0.5 lb/ton (0.23 kg/t) molten steel.

(*b*) *Commercial* CrMoV *steels*

	C	Cr	Mo	V	Mn	Si	S	Al	Ni	P	As	Sn	Sb	Cu	
CMV1	0.12	0.45	0.56	0.26	0.61	0.20	0.019	< 0.01	0.08	0.027	0.013	0.010	0.0025	0.08	all alloys: Nb, Ti, W < 0.01; Co < 0.02; B < 0.001
CMV3	0.13	0.48	0.53	0.21	0.50	0.33	0.023	< 0.01	0.33	0.019	0.032	0.010	0.003	0.14	
CMV4	0.12	0.31	0.65	0.25	0.60	0.26	0.017	< 0.01	0.31	0.018	0.032	0.021	0.0035	0.21	
CMV5	0.15	0.43	0.53	0.25	0.59	0.18	0.018	< 0.01	0.08	0.020	0.025	0.015	0.0025	0.15	
CMV6	0.10	0.46	0.56	0.24	0.55	0.19	0.023	< 0.01	0.14	0.031	0.021	0.010	0.004	0.14	
CMV7	0.11	0.42	0.54	0.30	0.60	0.34	0.020	< 0.01	0.05	0.018	0.033	0.010	0.002	0.03	
KDB	0.12	0.36	0.51	0.30	0.42	0.25	0.011	< 0.01	0.05	0.009	0.010	0.010	0.003	0.11	
HQE	0.13	0.39	0.43	0.26	0.55	0.20	0.012	< 0.01	0.15	0.010	0.020	0.012	0.005	0.12	
HZC†	0.10	0.15	0.66	0.25	0.63	0.25	0.018	< 0.01	0.10	0.018	0.015	0.120	0.0075	0.18	
TV0019†	0.10	0.68	0.75	0.34	0.55	0.26	0.011	< 0.01	0.022	0.016	0.014	0.010	0.003	0.15	
ESV0023†	0.13	0.70	0.71	0.35	0.54	0.28	0.011	< 0.01	0.19	0.009	0.016	0.010	0.003	0.15	

† Susceptible to h.a.z. cracking.

Tensile specimens (11.28 mm diameter; 25 mm gauge length) were heat treated and tested in vacuum (1.0–0.1 kPa) by using a machine equipped with r.f. induction heating and water-cooled loading bars to produce rates of heating and cooling sufficiently rapid to resemble those in the h.a.z. of a weld. Grain coarsened bainitic structures characteristic of those known to be susceptible to cracking were produced by a single cycle to 1300 °C with 10 s isothermal hold, followed by cooling to room temperature. Refined structures were produced by a subsequent cycle to 950 °C for 0.5 h to ensure complete transformation to fine grained austenite. The resulting prior austenite grain sizes and microstructures are summarized in table 2.

TABLE 2. SUMMARY OF GRAIN SIZE AND MICROSTRUCTURE: TENSILE SPECIMENS

	prior austenite grain size			ferrite
alloy	ASTM	mm	microstructure	(%)
(i) Grain-coarsened microstructures (1300 °C)				
experimental alloys				
'pure'	1–2	0.25–0.18	fully bainitic	0
P	1–2	0.25–0.18		
As	2–3	0.18–0.13		
Sn	0–1	0.35–0.25		
Sb	1–3	0.25–0.13		
(P, As, Sn, Sb)	0–1	0.35–0.25		
Cu	0–1	0.35–0.25		
commercial steels				
CMV1	0–1	0.35–0.25	pro-eutectoid	6.0
CMV3	1–2	0.25–0.18	ferrite at	4.0
CMV4	1–2	0.25–0.18	some prior	1.0
CMV5	0–1	0.35–0.25	austenite grain	4.0
CMV6	0–1	0.35–0.25	boundaries	10
CMV7	1–2	0.25–0.18		3.0
HQE	0–1	0.35–0.25		5.0
KDB	0–1	0.35–0.25	fully bainitic	0
HZC	1–2	0.25–0.18		
TV0019	1–2	0.25–0.18		
ESV0023	1–2	0.25–0.18		
(ii) Refined structures (1300/950 °C)				
'pure'	5–6	0.06–0.04	fully bainitic	0
(P, As, Sn, Sb)	5–6	0.06–0.04		
CMV3	7–8†	0.03–0.02	ferrite–bainite aggregate	50

† Mean ferrite–bainite grain size.

Specimens were tested at 550 °C at a nominal strain rate of 10^{-5}/s either in the untempered conditions or after tempering for 3 h or 10 h at 700 °C to produce variations in matrix strength comparable with those resulting from post weld heat treatment.

(*b*) *High temperature crack growth*

Studies of high temperature crack growth were carried out on four commercial steels of differing residual element content (i.e. CMV1, CMV3, CMV4 and HZC; table 1*b*) in microstructural conditions comparable with those of the tensile specimens.

Single edge notched tension specimens; (width (w) 20 mm; thickness (B) 12 mm) were tested

at constant load at 565 °C in vacuum. All specimens were notched to an initial depth (a) of 4 mm ($a/w = 0.2$) and crack extension was monitored by a direct current potential drop technique: specimen displacements accompanying crack growth were also measured in some tests.

For the grain coarsened specimens a load of approximately 14 kN was used (equivalent to an initial nominal linear elastic stress intensity of 9 $MNm^{-\frac{3}{2}}$, although this should not be taken to imply an expected correlation of crack growth rate with this parameter). Higher loads were necessary for some of the grain refined specimens. A post-test calibration of the potential drop data was made by measurements of actual crack length on specimens unloaded prior to failure at $a/w \approx 0.5$. This corresponded to more than 90 % of rupture life for the grain coarsened specimens, which exhibited a rapid onset of unstable growth at $a/w \gtrsim 0.4$.

4. Results

(a) *High temperature strength and ductility*

(i) *Grain coarsened structures*

Figures 1 and 2 show the effects of tempering at 700 °C on the 0.2 % proof stress and fracture elongation of the experimental alloys in the grain coarsened condition at 550 °C. It is apparent that, whereas the strengths were comparable (figure 1), there were large differences in ductility

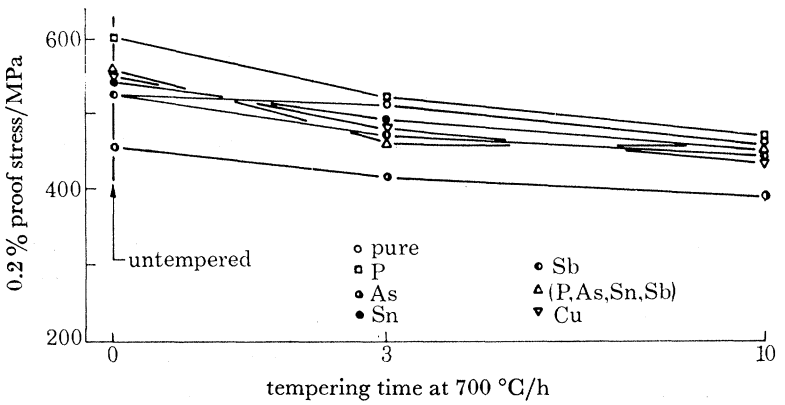

Figure 1. Effect of tempering on proof stress: experimental alloys; coarse-grained structures. $T = 550$ °C; $\dot{\epsilon} = 10^{-5}$/s.

which were accentuated by tempering. Thus, in contrast to the behaviour of the 'pure' alloy, the ductilities of the As, Sn, Sb and 'impure' alloys were low in the untempered condition and remained so after tempering (figure 2). The intermediate behaviour of the P and Cu alloys is noteworthy: the comparatively high ductility of the former increased at a rate more typical of the other impurity-containing alloys whereas the low initial ductility of the Cu alloy recovered with tempering at a similar rate to that of the 'pure' material.

As indicated in figure 2, the mode of failure was related to ductility such that for elongations less than about 5.5 % the failure path followed the prior austenite boundaries. For greater elongations there was a progressive replacement of the brittle, intergranular, mode by a more ductile process involving the plastic nucleation and growth of voids on inclusions within the matrix and on grain boundaries. Thus, in contrast to the P, Cu and 'pure' alloys which

exhibited transitions from intergranular to more ductile failures with tempering (figure 3, plate 1) the alloys containing As, Sn and Sb sustained intergranular fractures over the entire range (figure 4, plate 1). Individual grain faces on the fracture surfaces in the latter group showed clear evidence of cavities characteristic of those commonly observed under creep conditions at lower stresses and longer times and is indicative of cavitation as the operative mechanism of intergranular failure.

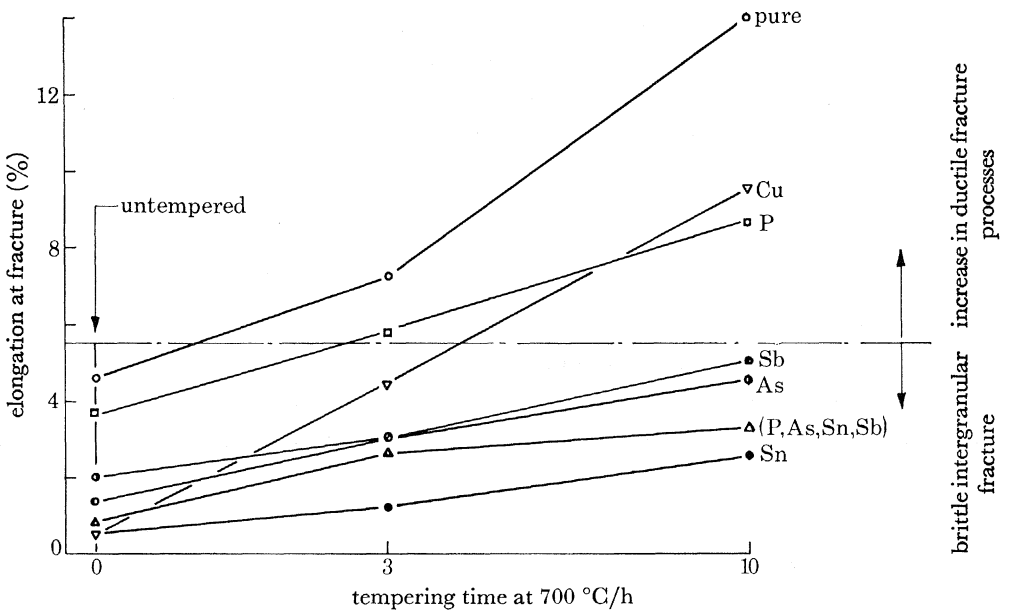

FIGURE 2. Effect of tempering on fracture elongation: experimental alloys; coarse-grained structures. $T = 550$ °C; $\dot{\epsilon} = 10^{-5}$/s.

Corresponding data for the commercial steels are shown in figures 5 and 6. In common with the experimental alloys, these were of similar strength (figure 5) but varied widely in ductility (figure 6), especially after tempering. By comparison with the behaviour of the experimental alloys (as indicated by the shaded area in figure 6) it is apparent that the range was at least as great and that a number of the commercial steels showed little improvement with tempering. It is significant that most of the steels in this latter group are known to be susceptible to stress relief cracking (i.e. HZC, TV0019, ESV0023).

The prior austenite grain sizes of all of the experimental alloys and commercial steels were within the overall range ASTM 0–3 (0.35–0.125 mm) while, for a given material, the variation was generally within one ASTM unit (table 2). Although the microstructures of all of the experimental alloys consisted entirely of granular bainite, some of the commercial steels differed in an important respect. Thus, while KDB, HZC, TV0019 and ESV0023 were fully bainitic, the remainder contained small quantities of proeutectoid ferrite at some of the prior austenite boundaries, varying from about 1% by volume (CMV4) to a maximum of 10% (CMV6) with most samples in the range 3–6% (table 2).

(ii) *Refined structures*

The effects of grain refinement were examined in three materials: the 'pure' and 'impure' experimental alloys and CMV3. All showed improved ductility (figure 7) and it should be

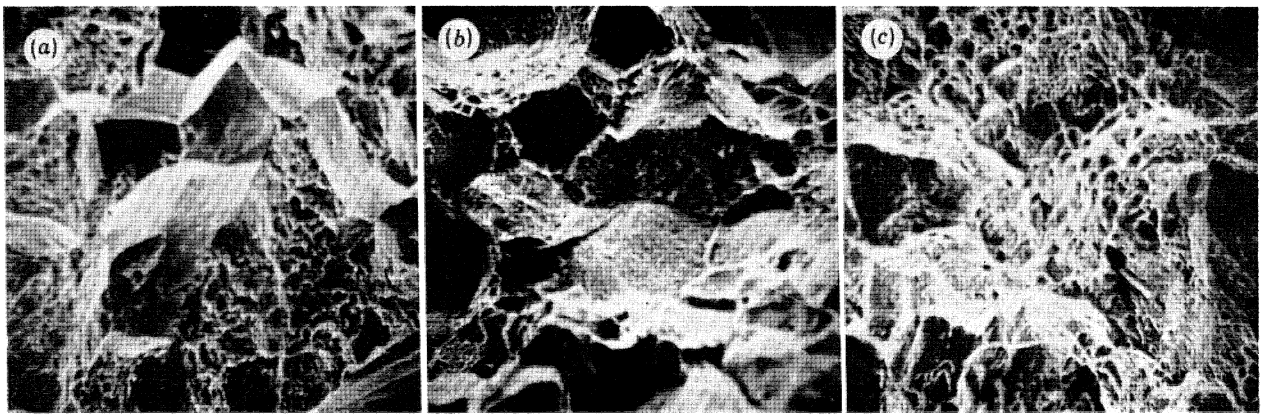

FIGURE 3. Transition to ductile fracture with tempering in 'pure' alloy. (*a*) 10 s at 1300 °C, untempered; (*b*) 10 s at 1300 °C, 3 h at 700 °C; (*c*) 10 s at 1300 °C, 10 h at 700 °C. (Magn. × 150.)

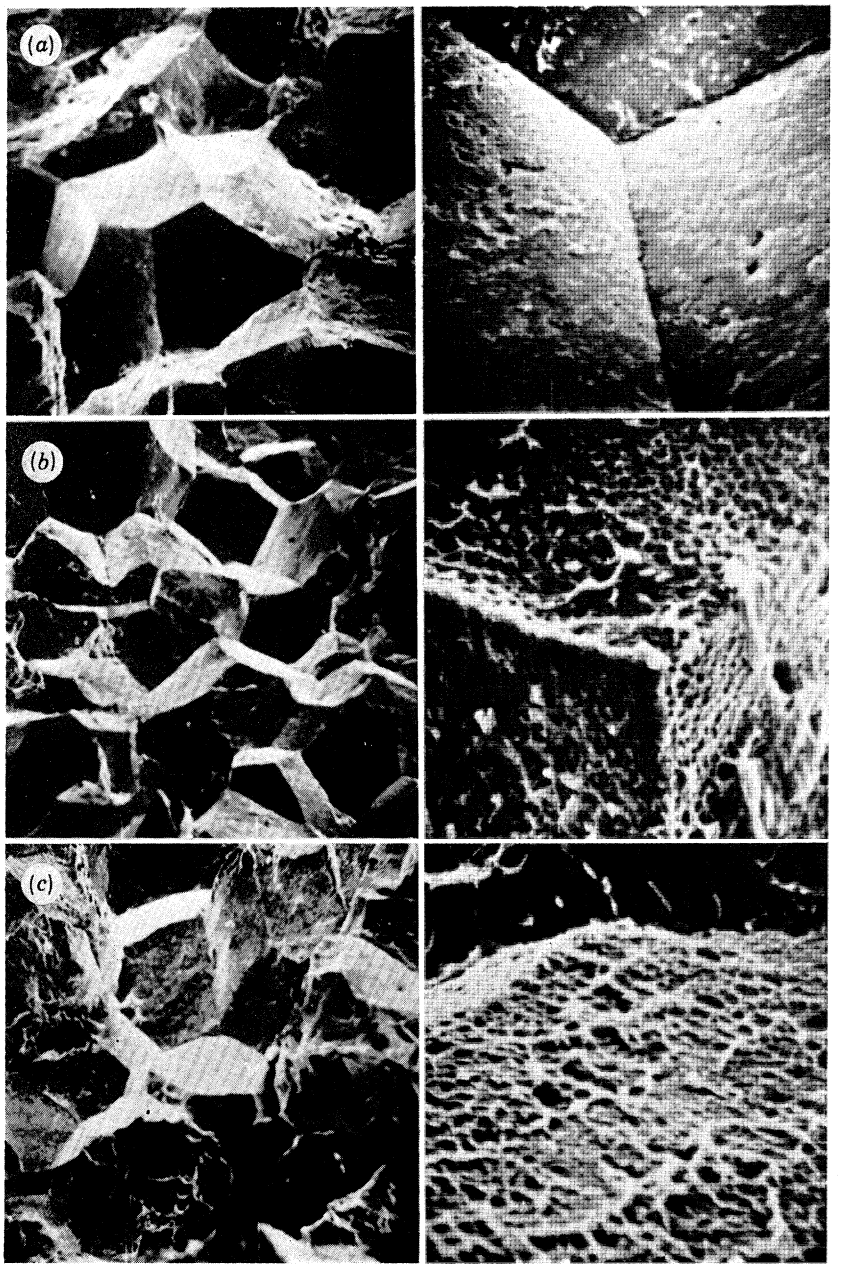

FIGURE 4. Persistence of intergranular fracture with tempering in Sn alloy. (*a*) 10 s at 1300 °C, untempered; (*b*) 10 s at 1300 °C, 3 h at 700 °C; (*c*) 10 s at 1300 °C, 10 h at 700 °C. (Magns: left, × 150; right, × 1500).

(*Facing p.* 240)

PHILOSOPHICAL TRANSACTIONS OF THE ROYAL SOCIETY A MATHEMATICAL, PHYSICAL & ENGINEERING SCIENCES

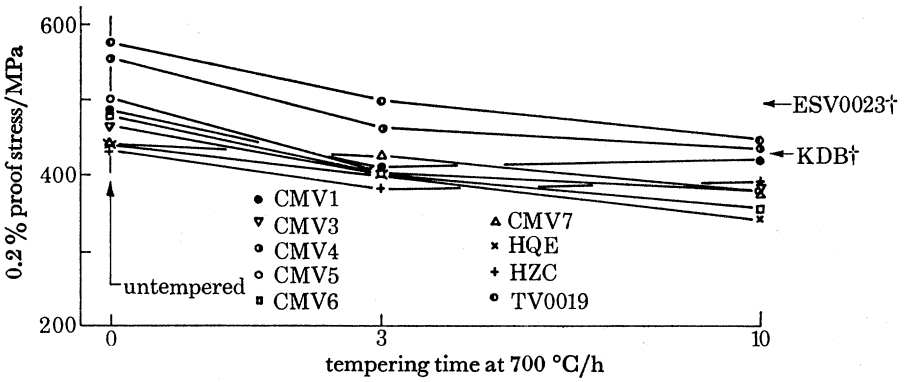

FIGURE 5. Effect of tempering on proof stress: commercial steels; coarse-grained structures. $T = 550$ °C; $\dot{\epsilon} = 10^{-5}$/s. † Tested 10 h at 700 °C only.

noted that the refined structure in the 'impure' alloy was superior to the grain coarsened 'pure' material in this respect.

The refined structures of both of the experimental alloys were fully bainitic and of comparable strength to the corresponding grain coarsened structures (i.e. within the range shown in

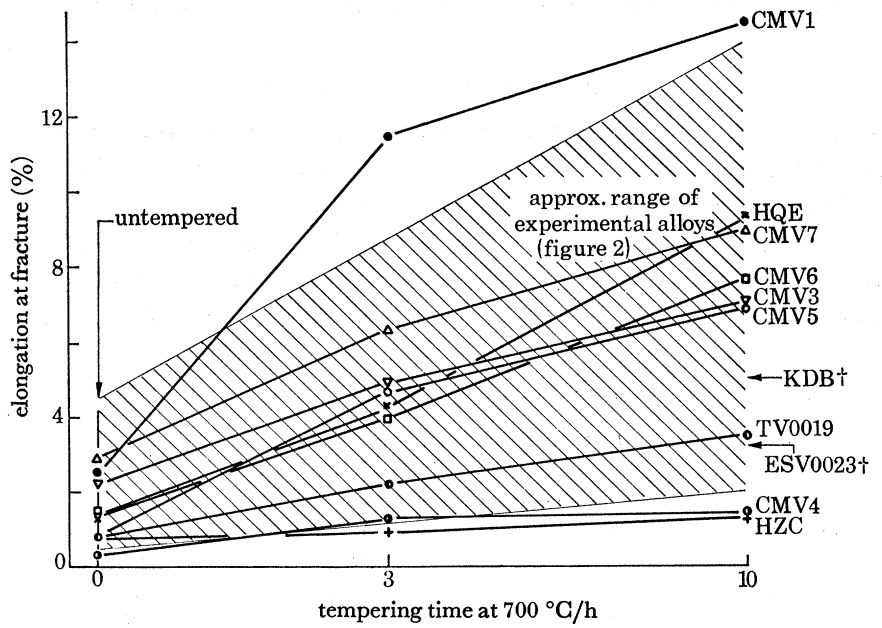

FIGURE 6. Effect of tempering on fracture elongation: commercial steels; coarse-grained structures. $T = 550$ °C; $\dot{\epsilon} = 10^{-5}$/s. † Tested 10 h at 700 °C only.

figure 1) and it is likely, therefore, that the improved ductility is largely a consequence of the reduction in prior austenite grain size (ASTM 5–6; table 2).

The structure of CMV3, on the other hand, consisted of approximately equal proportions of ferrite and bainite and, consequently, was about 30 % weaker than the coarse-grained material. Thus, in contrast to the experimental alloys, the improved ductility cannot be unambiguously attributed to grain refinement as the presence of ferrite will also be beneficial.

PHILOSOPHICAL TRANSACTIONS OF THE ROYAL SOCIETY A MATHEMATICAL, PHYSICAL & ENGINEERING SCIENCES

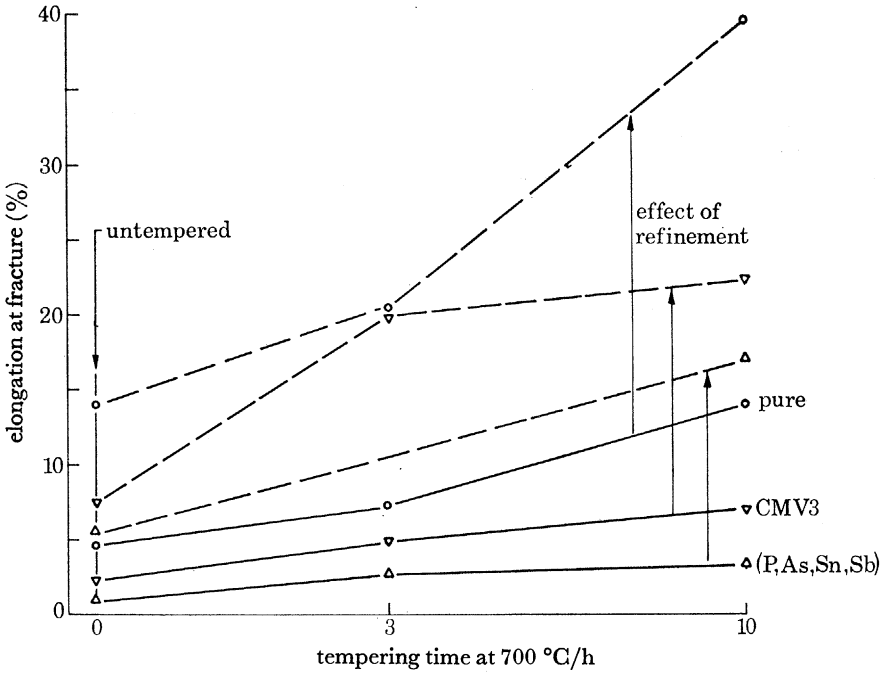

FIGURE 7. Effect of grain refinement on ductility. $T = 550$ °C; $\dot{\epsilon} = 10^{-5}$/s.

(*b*) *High temperature crack growth*

Results of crack growth tests at 565 °C are summarized in table 3 and figure 8. Although the prior austenite grain sizes were similar to the corresponding tensile specimens, the microstructures of all of the crack growth specimens were fully bainitic.

For the grain-coarsened structures in steels CMV1, CMV3 and CMV4 there was a consistent effect of tempering on both the rate of crack growth and time to failure. In addition, for a given degree of tempering, there were large differences in growth rate and failure time between the

TABLE 3. CRACK GROWTH TESTS AT 565 °C: SUMMARY OF RESULTS

	tempering time at 700 °C/h	crack growth rate, $\dot{a}$/(m/h)	failure time/h
	(i) Grain coarsened structures (1300 °C)		
CMV1	0	1.8×10^{-6}	1200
	10	1.5×10^{-7}	> 8000
CMV3	0	3.9×10^{-5}	45
	3	1.4×10^{-5}	130
	10	4×10^{-6}	620
CMV4	0	2×10^{-4}	10
	10	2.8×10^{-5}	70
HZC	3	1.8×10^{-4}	12
	(ii) Refined structures (1300/950 °C)		
CMV1	10	7×10^{-9}	N.A.
CMV4	10	2.4×10^{-6}	N.A.

All constant load tests were at $K_{\text{initial}} = 9\text{MN m}^{-\frac{3}{2}}$ except for refined structures which were step loaded. Failure times for the refined structures are consequently not applicable. Crack growth rates are given above for $K = 10\text{MN m}^{-\frac{3}{2}}$.

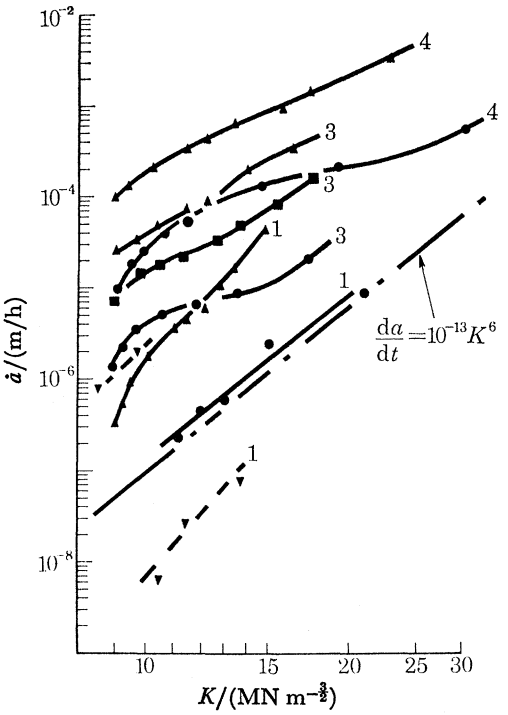

FIGURE 8. Summary of crack growth data for CrMoV steels at 565 °C: 1, CMV1; 3, CMV3; 4, CMV4. Coarse-grained bainitic structures: ▲, untempered; ■, 3 h at 700 °C; ●, 10 h at 700 °C. Refined structures: ▼, 10 h at 700 °C.

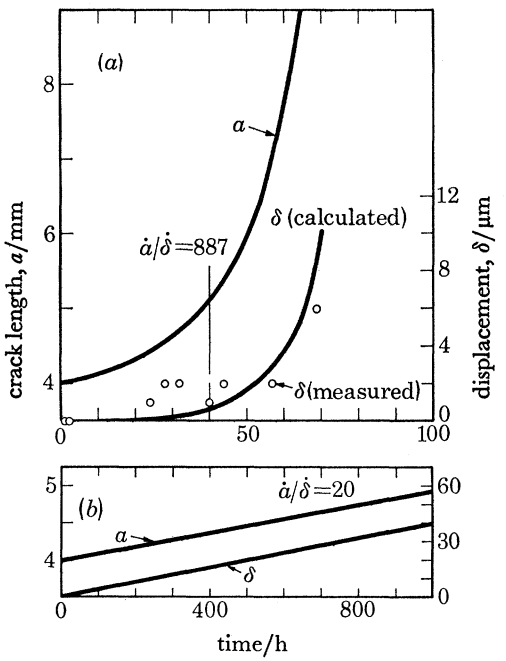

FIGURE 9. Effect of microstructure on crack growth and specimen displacement. (*a*) Coarse-grained bainite; $\delta = \frac{1}{\sqrt{3}}K^2/\sigma yE$. (*b*) Refined bainite.

three steels. However, despite the wide range of growth rates (about three orders of magnitude) measured in the grain-coarsened structures, all showed characteristic acceleration of crack growth rate from the onset of the test, as typified by data for CMV4 in figure 9. In these structures crack extension occurred by the nucleation, growth and linkage of creep cavities on the prior austenite grain boundaries ahead of the tip of the crack. This damage accumulation process was localized to a band less than 50 μm in width and is consistent with the small displacements accompanying crack growth, as typified by figure 9.

Crack growth rates for the refined structures were lower than for the corresponding grain-coarsened specimens (table 3; figure 8); however, differences in growth rate between CMV1 and CMV4, consistent with those noted above, were also observed. In contrast to the grain-coarsened structures, the refined specimens exhibited prolonged periods of stable behaviour where crack length and displacement increased at constant rates (figure 9). The large differences in displacement between the corresponding coarse and refined structures is particularly significant and is consistent with the differences in ductility described in the previous section.

5. Discussion

It is apparent from the preceding results that residual impurity elements and grain refinement both exert a strong influence on the high temperature ductility and crack growth behaviour of bainitic structures. These two factors and their practical implications will now be considered.

(*a*) *Intergranular embrittlement by residual elements*

The reduction in ductility and concomitant transition to intergranular fracture at a given strength level (figure 10) in the impurity doped grain coarsened experimental alloys is clear evidence that Sb, Sn, As and, to a lesser extent, Cu reduce the cohesive strength of prior austenite grain boundaries and promote high temperature brittleness. The present results permit the specific effect of each element to be evaluated. Thus, based on the fracture elongation data for material tempered at 700 °C for 10 h (figure 2) it is possible to rank the impurities in the following order of severity:

element	P	As	Sn	Sb	Cu
severity (mass %)	1.0	2.43	3.57	8.16	0.13
(at. %)	1.0	5.88	13.7	32.1	0.27

Although Cu has been included above, it should be noted that, whereas the relative effects of P, As, Sn and Sb were similar for other material conditions, its effect diminished with tempering indicating a different mechanism of embrittlement.

In common with the experimental alloys the commercial CrMoV steels exhibited a wide range of ductility at a given strength level (figure 11) and also showed clear evidence of intergranular embrittlement. Although these steels contained differing levels of P, As, Sn and Sb it was possible to relate their ductility to the effective residual element content, given by

$$R = [\mathrm{P}] + 2.43[\mathrm{As}] + 3.57[\mathrm{Sn}] + 8.16[\mathrm{Sb}],$$

where concentrations are expressed in percentages by mass, assuming that the effect of each element is proportional to the amount present and that their separate effects are additive. Figure 12 shows fracture elongation of the experimental alloys and commercial steels in the fully tempered (700 °C/10 h) condition as a function of R and two similar plots are evident. One

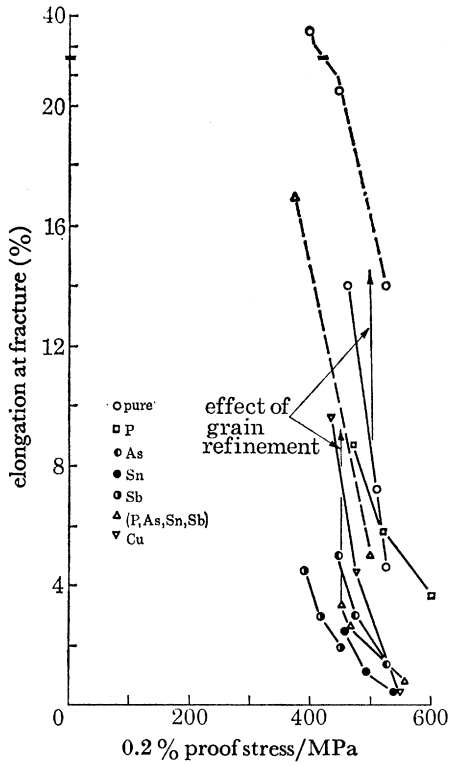

FIGURE 10. Relations between strength and ductility: experimental alloys. ——, Grain-coarsened (1300 °C); – – –, refined (1300/950 °C). $T = 550$ °C; $\dot{\epsilon} = 10^{-5}$/s.

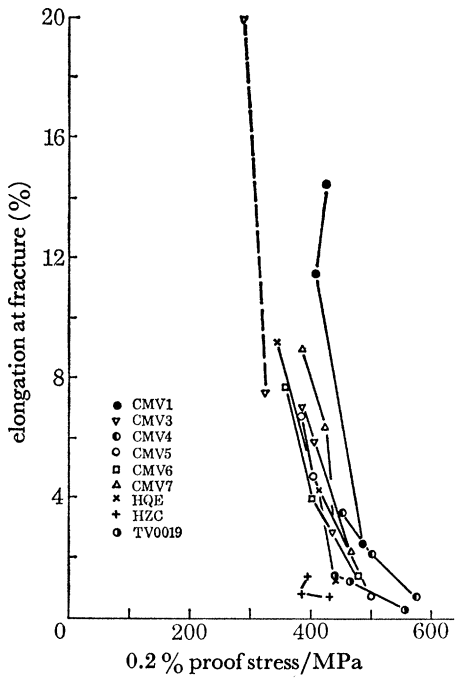

FIGURE 11. Relations between strength and ductility: commercial steels. ——, Grain-coarsened (1300 °C); – – –, refined (1300/950 °C). $T = 550$ °C; $\dot{\epsilon} = 10^{-5}$/s.

comprises points for the experimental alloys and also includes the fully bainitic commercial steels of corresponding microstructure. This falls to a lower ductility plateau at $R \lesssim 0.11$ and is indicative of a saturation effect. The other, which comprises the data points for the ferrite containing commercial steels, although parallel to that above, is displaced to higher residual element levels such that the lower ductility plateau is reached at $R \approx 0.2$. As the materials in both groups were of comparable grain size the displacement of the latter plot to higher residual levels is clearly indicative of the beneficial effect of small amounts of pro-eutectoid ferrite at prior austenite boundaries on high temperature ductility and on the tolerance to residual elements. An analogous effect of pro-eutectoid ferrite on high temperature crack growth has recently been described by Gooch (1977).

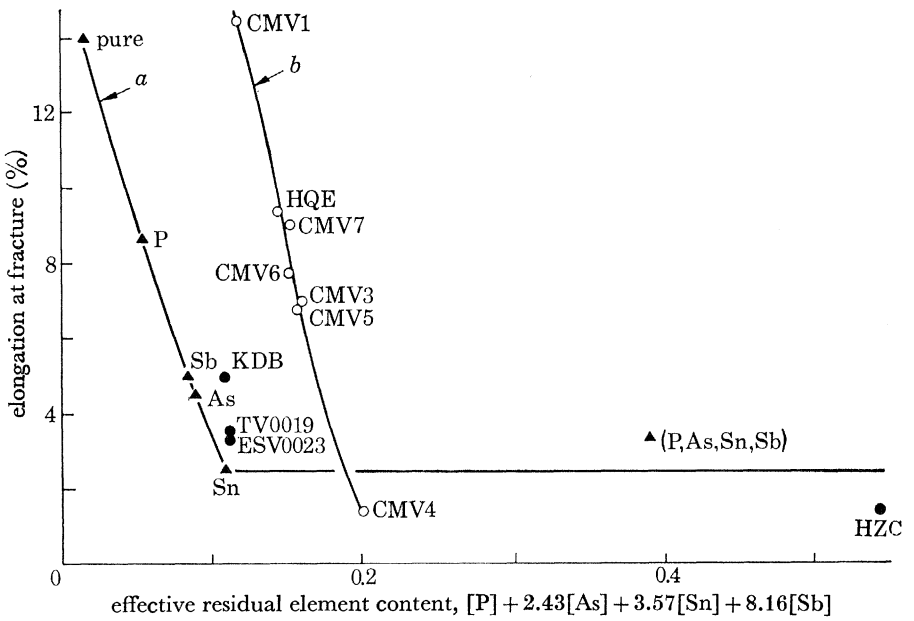

FIGURE 12. Relation between ductility and residual element content; coarse-grained structures, tempered 10 h at 700 °C, tested at 550 °C, $\dot{\epsilon} = 10^{-5}$/s. (*a*) Experimental alloys (fully bainitic); (*b*) commercial steels (ferrite–bainite).

It is clear from this work that, for a given microstructural condition, the high temperature ductility can be related to the residual element content by using the weighting factors derived from the work on controlled purity materials.

It is also possible to rationalize high temperature crack growth rates in terms of the effective residual element content in grain-coarsened structures. In common with the mode of failure observed in tensile tests the mechanism of crack growth was observed to involve similar processes, i.e. the nucleation, growth and linkage of cavities on prior austenite boundaries ahead of the tip of the crack. On this basis, figure 13 shows crack growth rates at a given stress as a function of R. It is clear that a similar relation to that described above for tensile ductility also exists for high temperature crack growth in the materials examined.

Intergranular embrittlement occurs when the effective surface energy of the operative mode of grain boundary failure is reduced below that of any other fracture process. In general, this could result from the effect of an external environment, as in the case of stress corrosion cracking,

or from the segregation of certain elements from the matrix to the grain boundaries, as in temper embrittlement. Thus the high temperature embrittlement phenomenon considered here shares a number of features with temper embrittlement although the detailed grain boundary failure mechanisms are obviously different. It is significant that the present embrittlement ranking order for P, As, Sn and Sb, in common with that recently determined for stress relief embrittlement in MnNiMo (ASME A533B) pressure vessel steels (Brear & King 1976 and this symposium), is similar to that previously determined by Low *et al.* (1964) for temper embrittlement in NiCr steels, the principal difference being the comparatively small effect of P in the present work. Consequently it will be assumed that embrittlement is the result of segregation of

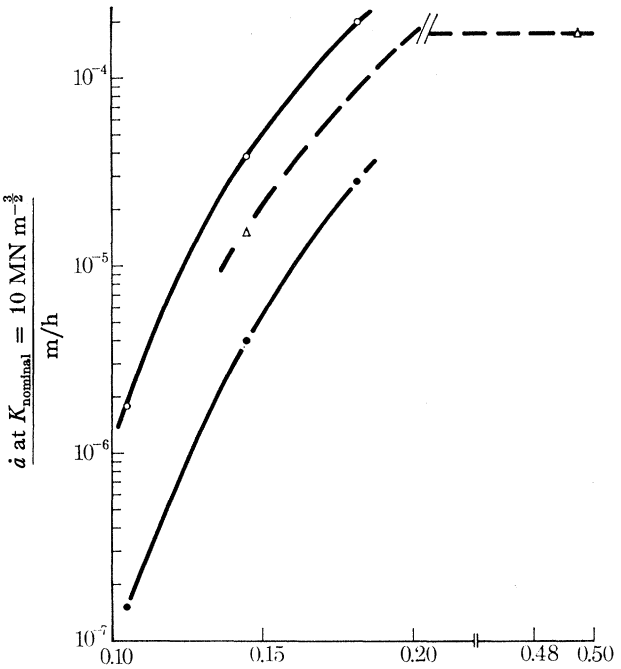

FIGURE 13. Effect of composition on crack growth rates in $\frac{1}{2}$Cr$\frac{1}{2}$Mo$\frac{1}{4}$V steels tested at 565 °C; 10 s at 1300 °C, oil quenched. ○, untempered; △, tempered 3 h at 700 °C; ●, tempered 10 h at 700 °C.

impurity atoms to prior austenite grain boundaries during high temperature exposure in the ferrite phase, i.e. during thermal equilibration and elastic loading in the tensile tests at 550 °C and also during prior ageing at 700 °C in the case of the tempered specimens.

The degree of embrittlement caused by an impurity species reflects the combined effect of a number of factors, namely the driving force for segregation, the mobility of the species in the matrix and its effect on the fracture energy of the grain boundary. Solute segregation to grain boundaries has been examined by McLean (1957) who showed that the equilibrium concentration C of solute at a boundary is related to the bulk concentration, C_{L}, such that:

$$C = AC_{\mathrm{L}}\mathrm{e}^{E/RT}/(1 + AC_{\mathrm{L}}\mathrm{e}^{E/RT}).$$

A is a factor which accounts for changes in vibrational entropy in the boundary region and E is the decrease in energy accompanying the transfer of an atom of solute from the lattice to a boundary site. Thus, at a given temperature the grain boundary solute content depends strongly on the driving force for segregation, E. If it is assumed that the driving force is derived

mainly from lattice misfit strains and that these are zero for a solute in the boundary then the maximum value of E will be the elastic strain energy associated with a substitutional solute atom in the α-Fe lattice given by

$$E_{\max} = 6\mu\Omega\epsilon^2$$

(Nabarro 1940), where μ and Ω are the shear modulus and atomic volume of α-Fe and ϵ is the elastic strain produced by a solute atom. Relative values of ϵ can be determined from the effect of each impurity on the lattice parameter of α-Fe. Thus of the solutes considered, Sb causes the greatest misfit and P the least, as summarized in table 4. These values may be compared with the observed embrittlement severities (table 5). It is noteworthy that the predicted ranking order for segregation driving force is the same as that observed for embrittlement. However, little emphasis should be given to the numerical factors for the former as the assumption of zero misfit for a solute atom at a grain boundary is unrealistic and because other factors which might cause segregation, e.g. chemical interactions, have been ignored.

TABLE 4. LATTICE STRAINS IN α-Fe SOLID SOLUTIONS

element	$10^4\epsilon$†	$10^8\epsilon^2$	$\epsilon^2/\epsilon_p^2 = E/E_p$	Reference
P	−2.79	7.79	1.0	Pearson (1967)
As	9.76	95.4	12.5	
Sn	22.7	514	66	Speight (1972)
Sb	29.7	879	113	Predel & Frebel (1971)

† For 1 atom % solute

TABLE 5. RELATIVE EMBRITTLEMENT SEVERITY

element	mass percentage	atomic percentage	E/E_p
P	1.0	1.0	1.0
As	2.43	5.88	12.5
Sn	3.57	13.67	66
Sb	8.16	32.07	113

However, in most practical situations the degree of segregation will be determined by the kinetics of the process and the diffusivity D of the solute. As the approach to equilibrium is slow, a useful parameter is the time required to attain a grain boundary concentration equal to half the equilibrium value, given by

$$t_{\frac{1}{2}} = 9\alpha^2 d^2/64D$$

(McLean 1957), where $\alpha = C/C_L$ and d is the width of the grain boundary region. For phosphorus segregation in 3CrMo steel at 550 °C, measured and predicted values of $t_{\frac{1}{2}}$ were shown to be 0.90 and 0.94 h respectively (King & Wigmore 1976). Thus, as the period at temperature before the onset of plastic strain in the present tensile tests was typically 1.5–2 h, it is clear that sufficient time was available to allow significant phosphorus segregation.

Comparative diffusion data for P, As, Sn and Sb in α-Fe at 550 °C are not available but their diffusion coefficients at 800 °C are similar (table 6). Therefore, provided a similar situation prevails at 550 °C, substantial segregation of As, Sn and Sb could also have occurred.

The dominant mechanism of intergranular failure in these alloys was the growth and linkage of voids. It is likely, therefore, that the principal effect of segregated impurities is to enhance the

nucleation of voids by reducing the effective surface energy, γ, for their growth. Thus, if the criterion for stable void growth is:

$$r_c > 2\gamma/\sigma$$

a reduction in γ will reduce the critical void size at which stable growth will occur at a given stress, σ.

It has been previously observed (Middleton, this symposium) that voids nucleate heterogeneously on grain boundary particles. If these particles exhibit a distribution of sizes, then, for a given structural condition and matrix flow stress a reduction in γ caused by segregation will decrease r_c and increase the density of growing voids. This, in turn, will expedite intergranular failure by their diffusion controlled linkage and, thereby, lead to reduced ductility under constant strain rate deformation conditions and to increased rates of high temperature crack growth.

TABLE 6. DIFFUSION OF SOLUTES IN α-Fe (800–900 °C)

solute	$D_0/(\mathrm{cm}^2/\mathrm{s})$	$Q/(\mathrm{kJ/mol})$	$10^{11}D_{800\,^\circ\mathrm{C}}/(\mathrm{cm}^2/\mathrm{s})$	reference
P	7.1×10^{-3}	167	4.73	Gruzin & Minal (1963)
As	—	—	7.9	Yakushechkina *et al.* (1974)
Sn	2.4	221	3.5	Treheux *et al.* (1972)
Sb	440	270	2.75	
Fe (self-diffusion)	38	270	0.238	Bruggeman & Roberts (1975)

In the preceding discussion, particular attention has been given to the effects of P, As, Sn and Sb. However, the behaviour of the Cu alloy is also of interest as it may indicate a different mechanism of embrittlement. In this material the ductility in the as-transformed condition was low but increased with tempering at a rate comparable to that of the 'pure' alloy (figure 2). Such behaviour might be interpreted in terms of the dispersal of pre-segregated copper atoms from the boundaries during tempering at 700 °C. Because of the mobility of Cu is similar to that of self diffusion in α-Fe (Anand & Agarwala 1966) this clearly implies that segregation occurred in the austenite phase at 1300 °C. Although there is no direct evidence to support this suggestion, as for example from Auger electron spectroscopy, the work of Melford (1962, 1966) on 'hot shortness' in copper-containing mild steels provides circumstantial evidence that segregation may occur in austenite at temperatures above 1100 °C.

(*b*) *Residual element control as a means of preventing h.a.z. cracking*

The present work has shown that the ductility and resistance to crack growth of coarse-grained bainitic structures in CrMoV steels can be improved by restricting the levels of certain residual elements. It is likely therefore that residual element control will also provide improved resistance to cracking in CrMoV weldments during stress relief and in service.

Based upon the specific effects of the residual elements determined here it is clear that Sb is the most detrimental at a given level. However, the effective content of a particular impurity element depends upon the product of its weighting factor and the amount present. Thus, for the commercial CrMoV steels examined here (table 1*b*) it is apparent that Sn and As provide the greatest contributions to embrittlement. The absence hitherto of formal limits for As and Sb in specifications for CrMoV steels therefore represents a serious deficiency. This situation can obviously be remedied by assigning maximum values to all of the residual elements on the basis of weighting factors derived experimentally. However, it is significant that, with the exception

of P, none of the elements studied here can be removed by conventional steelmaking processes and the only effective means of control is through selection of raw materials such as ore and scrap. Moreover, high grade materials have been placed at a premium by the progressive decline in the purity of scrap, particularly with respect to Cu and Sn, which has resulted from recycling. The scarcity of these materials will be further exacerbated by the increasing awareness of the benefits of and need for residual element control in other areas of engineering. Important examples in the power industry alone are the control of temper embrittlement in l.p. turbine and alternator rotor forgings and the prevention of stress relief and irradiation embrittlement in plates and forgings for l.w.r. vessels. It is therefore to be expected that the cost of high purity materials will continue to rise at an increasing rate and in this situation more stringent restrictions on residual element content must be justified by corresponding benefits.

It is suggested that an alternative and more logical approach to residual element control would be to assign a maximum value to the effective residual element content, R, and to assess individual maxima for each element on the basis of specific manufacturing practice. For example, certain ores are known to yield As levels which, in themselves, might be considered unacceptably high (*ca.* 0.04% by mass). However, these materials are also consistently and sufficiently low in Sn and Sb to offset the high As level and maintain an acceptable value of R. It is considered that such an approach could form the basis of a more flexible and less costly system of residual element control better suited to the situation of increasing scarcity and expense of pure raw materials likely in future.

(*c*) *Grain refinement as a means of preventing h.a.z. cracking*

The present results show clearly that grain refinement is an effective means of increasing high temperature ductility and resistance to crack growth. In practical terms the observation that, in the experimental alloys, the ductility of the refined 'impure' material was greater than that of the grain-coarsened 'pure' alloy (figure 7) is of particular importance since it shows clearly that grain refinement can provide a more effective means of improving h.a.z. ductility than residual element control *per se*. The economic implications are also important since in the long term the refinement of weldment microstructures will be less costly than residual element control. These observations are not confined to CrMoV steels and a similar situation has been shown to exist in the MnNiMo pressure vessel steels (ASME A533B/A508 class 3) (Brear & King 1976).

Microstructure control during welding appears to provide an effective and economically attractive means of providing increased tolerance to residual elements in CrMoV steels and its practical implementation is being pursued in the U.K. power industry. However, until this is achieved careful control of residual element levels must continue to be exercised.

6. Conclusions

1. The presence of P, As, Sn and Sb promotes high temperature intergranular embrittlement in CrMoV steels and is detrimental to ductility and creep crack growth. These elements increase the risk of heat affected zone cracking during stress relief and in service.

2. The relative importance of these elements has been identified. For a given mass fraction the relative embrittlement severities are in the following order: P(1), As(2.43), Sn(3.57), Sb

(8.16). This order is consistent with that predicted for segregation driving force, based on the lattice strain of each solute in α-Fe.

3. The high temperature ductility and crack growth behaviour of commercial $\frac{1}{2}C\frac{1}{2}Mo\frac{1}{4}V$ steels can be related to the weighted sum of the P, As, Sn and Sb levels by using the factors above.

4. The presence of Cu is most detrimental in the untempered condition. In fully tempered material its specific effect is small in comparison with the other elements.

5. Although the specific effect of Sb is greatest, significant embrittlement can also be caused by As and Sn because of the relatively high level often present in commercial CrMoV steels. Particular attention should, therefore, be given to the control of all of these elements.

6. Grain refinement is beneficial to high temperature ductility and resistance to crack growth. This provides an effective practical means of improving the tolerance of CrMoV steels to residual elements.

7. Residual element and microstructure control should be regarded as complementary, rather than alternative, means of preventing h.a.z. cracking. Compositional standards should not, however, be relaxed until reliable control of h.a.z. microstructure can be achieved in practice.

The work was carried out at the Central Electricity Research Laboratories and the paper is published by permission of the Central Electricity Generating Board.

References (King)

Anand, M. S. & Agarwala, R. P. 1966 *J. appl. Phys.* **37**, 4248.
A.S.T.M. 1968 *Temper embrittlement in steel.* S.T.P. 407.
A.S.T.M. 1971 *Temper embrittlement in alloy steels.* S.T.P. 499.
Batte, A. D., Miller, R. C. & Murphy, M. C. 1976 In *Brunchuntersuchungen und Schadenklärung*, pp. 173–180. Munich and Berlin: Allianz Versicjerungs-AG.
Brear, J. M. & King, B. L. 1976 In *Institution of Metallurgists Conference on Grain Boundaries*, Jersey, April 1976, pp. C13–C18.
Bruggeman, G. A. & Roberts Jr, J. A. 1975 *Metall. Trans.* A **6**, 755.
Gooch, D. J. 1977 *Mater. Sci. Engng.*, **27**, 57–68.
Gruzin, P. L. & Minal, V. V. 1963 *Fizika Metall.* **16** (4), 50–54.
Harris, P. & Jones, K. E. 1972 In *International Conference of Welding Research Related to Power Plant*, C.E.G.B., Southampton, Sept. 1972, p. 369.
Hopkins, B. E., Tipler, H. R. & Branch, G. D. 1971 *J. Iron Steel Inst.* **209** 745.
King, B. L. & Wigmore, G. 1976 *Metall. Trans.* A **7**, 1761.
Low Jr, J. R., Stein, D. F., Turkalo, A. M. & Laforce, R. P. 1968 *Trans. Am. Inst. metall. Petrol. Engrs* **242**, 14.
McLean, D. 1957 *Grain boundaries in metals.* Oxford University Press.
Melford, D. A. 1962 *J. Iron Steel Inst.* **200**, 290.
Melford, D. A. 1966 *J. Iron Steel Inst.* **204**, 495.
Myers, J. 1972 In *International Conference on Welding Research Related to Power Plant*, C.E.G.B., Southampton, Sept. 1972, p. 356.
Myers, J. & Price, A. T. 1977 *Metals Technol., Lond.* **4**, 406–410.
Nabarro, F. R. N. 1940 *Proc. phys. Soc.*, **52**, p. 90.
Pearson. W. B. 1967 *Handbook of lattice spacings and structures of metals and alloys*, vol 2. Pergamon Press.
Predel, B. & Frebel, M. 1971 *Arch. EisenhüttWes.* **42**, 365.
Schüller, H.-J., Hagn, L. & Woitscheck, A. 1974 *a Maschinenschaden* **47**, 1–13.
Schüller, H.-J., Christian, H. & Kober, A. 1974 *b Maschinenschaden* **47**, 19–74.
Speight, E. A. 1972 *Metal Sci. J.* **6**, 57.
Tipler, H. R. & Hopkins, B. E. 1976 *Metal Sci. J.* **10**, 47.
Treheux, D., Marchive, D., Delagrange, J. & Guiraldenq, P. 1972 *C. hebd. Séanc. Acad Sci., Paris* C **274**, 1260–1262.
Yakushechkina, L. I., Shumilov, M. A. & Yakushechkin. E. I. 1974 *Izv. vyssh. ucheb. Zaved. chern. Metall.* **4**, 116–119.

PHILOSOPHICAL TRANSACTIONS OF THE ROYAL SOCIETY A MATHEMATICAL, PHYSICAL & ENGINEERING SCIENCES

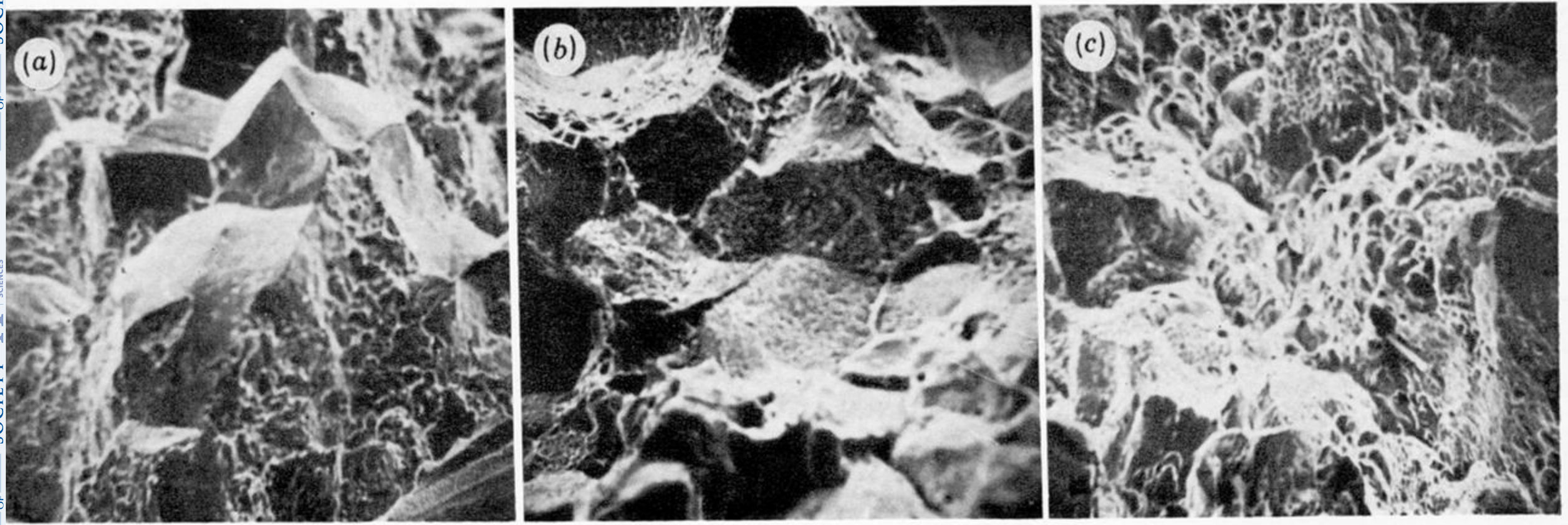

FIGURE 3. Transition to ductile fracture with tempering in 'pure' alloy. (*a*) 10 s at 1300 °C, untempered; (*b*) 10 s at 1300 °C, 3 h at 700 °C; (*c*) 10 s at 1300 °C, 10 h at 700 °C. (Magn. × 150.)

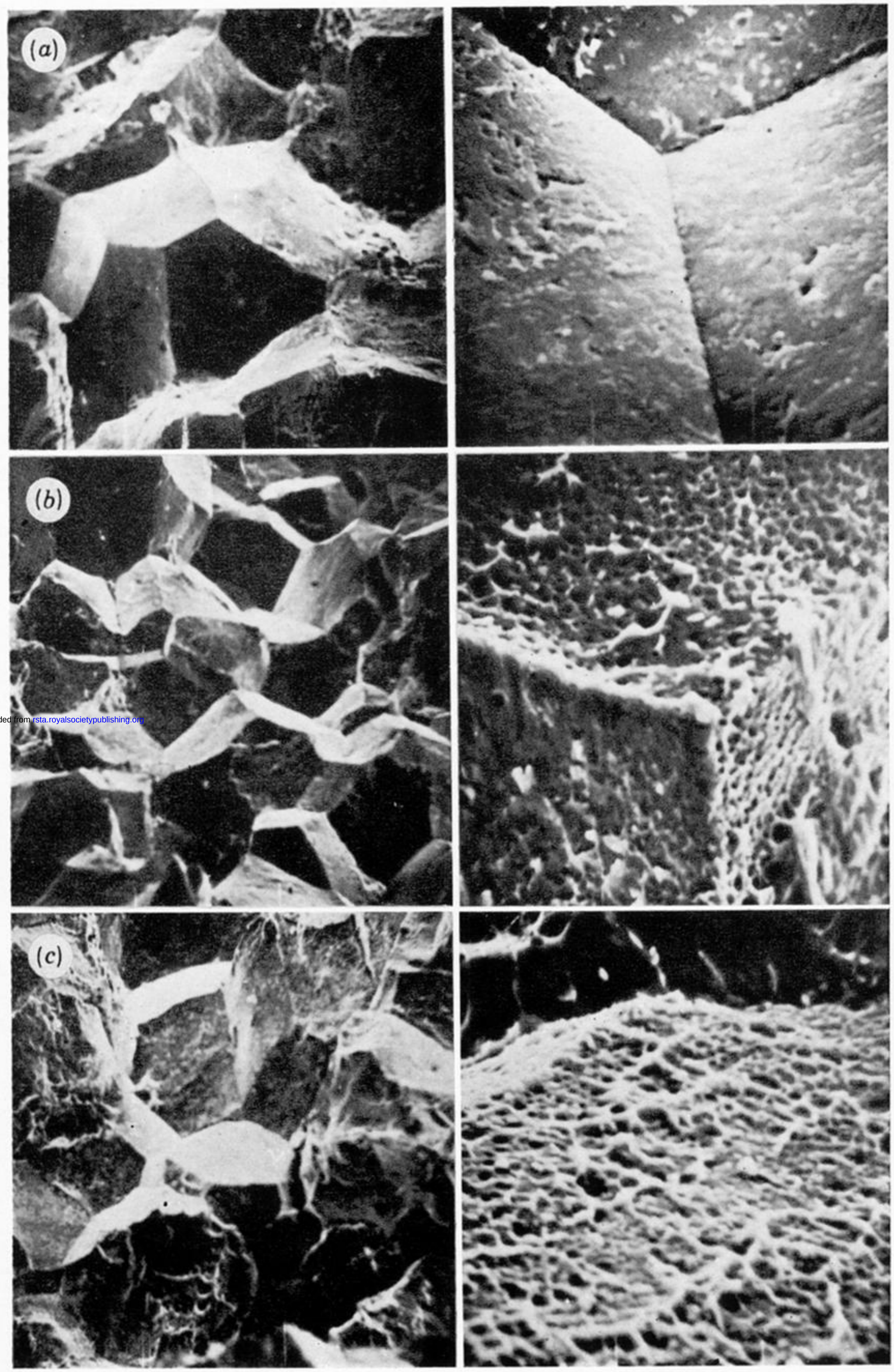

FIGURE 4. Persistence of intergranular fracture with tempering in Sn alloy. (*a*) 10 s at 1300 °C, untempered; (*b*) 10 s at 1300 °C, 3 h at 700 °C; (*c*) 10 s at 1300 °C, 10 h at 700 °C. (Magns: left, × 150; right, × 1500).